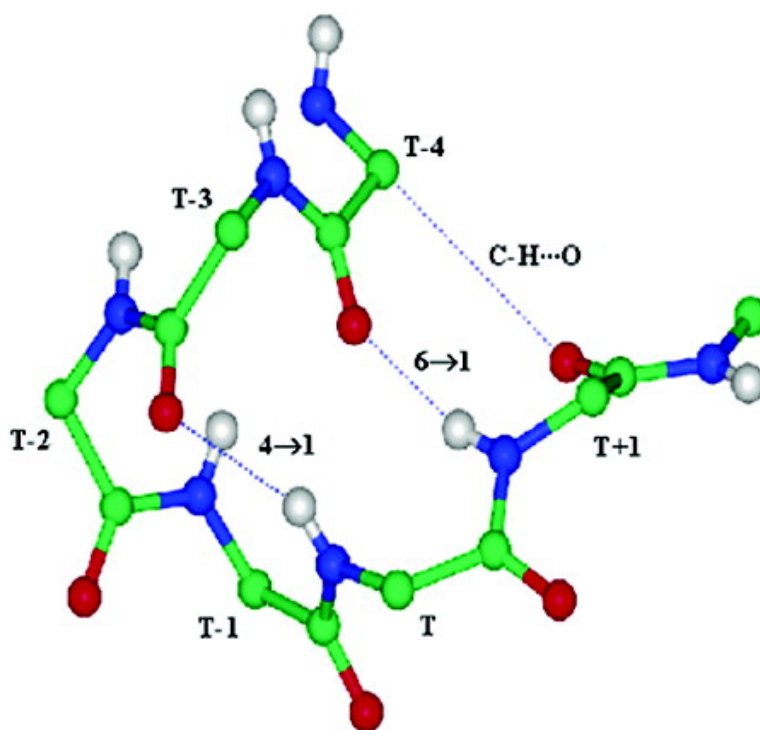


Probing the Role of the C–H...O Hydrogen Bond Stabilized Polypeptide Chain Reversal at the C-terminus of Designed Peptide Helices. Structural Characterization of Three Decapeptides

Subrayashastry Aravinda, Narayanaswamy Shamala, Abhishek Bandyopadhyay, and Padmanabhan Balaran

J. Am. Chem. Soc., **2003**, 125 (49), 15065-15075 • DOI: 10.1021/ja0372762 • Publication Date (Web): 13 November 2003

Downloaded from <http://pubs.acs.org> on March 30, 2009



More About This Article

Additional resources and features associated with this article are available within the HTML version:

- Supporting Information
- Access to high resolution figures
- Links to articles and content related to this article
- Copyright permission to reproduce figures and/or text from this article



[View the Full Text HTML](#)



Probing the Role of the C–H···O Hydrogen Bond Stabilized Polypeptide Chain Reversal at the C-terminus of Designed Peptide Helices. Structural Characterization of Three Decapeptides

Subrayashastry Aravinda,[†] Narayanaswamy Shamala,^{*,†}
Abhishek Bandyopadhyay,[‡] and Padmanabhan Balaram^{*,‡}

Contribution from the Department of Physics and Molecular Biophysics Unit,
Indian Institute of Science, Bangalore 560 012, India

Received July 15, 2003; E-mail: pb@mbu.iisc.ernet.in; shamala@physics.iisc.ernet.in

Abstract: The structural characterization in crystals of three designed decapeptides containing a double D-segment at the C-terminus is described. The crystal structures of the peptides Boc-Leu-Aib-Val-Xxx-Leu-Aib-Val-DAla-DLeu-Aib-OMe, (Xxx = Gly **2**, DAla **3**, Aib **4**) have been determined and compared with those reported earlier for peptide **1** (Xxx = Ala) and the all L analogue Boc-Leu-Aib-Val-Ala-Leu-Aib-Val-Ala-Leu-Aib-OMe, which yielded a perfect right-handed α -helical structure. Peptides **1** and **2** reveal a right-handed helical segment spanning residues 1 to 7, ending in a Schellman motif with DAla(8) functioning as the terminating residue. Polypeptide chain reversal occurs at residue 9, a novel feature that appears to be the consequence of a C–H···O hydrogen bond between residue 4 C^αH and residue 9 CO groups. The structures of peptides **3** and **4**, which lack the *pro R* hydrogen at the C^α atom of residue 4, are dramatically different. Peptide **3** adopts a *right-handed* helical conformation over the 1 to 7 segment. Residues 8 and 9 adopt α_L conformations forming a C-terminus type I' β -turn, corresponding to an incipient *left-handed* twist of the polypeptide chain. In peptide **4**, helix termination occurs at Aib(6), with residues 6 to 9 forming a left-handed helix, resulting in a structure that accommodates direct fusion of two helical segments of opposite twist. Peptides **3** and **4** provide examples of chiral residues occurring in the less favored sense of helical twist; DAla(4) in peptide **3** adopts an α_R conformation, while LVal(7) in **4** adopts an α_L conformation. The structural comparison of the decapeptides reported here provides evidence for the role of specific C–H···O hydrogen bonds in stabilizing chain reversals at helix termini, which may be relevant in aligning contiguous helical and strand segments in polypeptide structures.

Introduction

The use of α -aminoisobutyric acid (Aib) residues to generate helical peptide structures is well established.^{1,2} The availability of designed synthetic peptide scaffolds permits probing of the effect of introducing D-residues into sequences composed of largely L-amino acids, which are expected to fold into right-handed helical structures.³ Several years ago Charlotte Schellman noted that in proteins helix termination often occurs when a C-terminus residue, most frequently Gly, adopts a left-handed (α_L) conformation.⁴ The Schellman motif is characterized by a

pair of 6 \rightarrow 1 and 4 \rightarrow 1 intramolecular hydrogen bonds and has been widely observed in proteins.⁵ In model peptides, this motif have been observed, with achiral residues such as Aib adopting the α_L conformation near the C-terminus of largely helical peptides.⁶ Such local α_L -conformations ($\phi = +60^\circ$, $\psi = +30^\circ$) are also expected to be favored by D-residues. Thus, the introduction of D-residues into helical L-peptide sequences can, in principle, result in helix termination with the formation of a Schellman motif. During the course of systematic investigations of the effect of using D-residues in L-peptide helices, we began with the consideration of the parent all L-sequence Boc-Leu-

[†] Department of Physics.

[‡] Molecular Biophysics Unit.

- (1) (a) Prasad, B. V. V.; Balaram, P. *Crit. Rev. Biochem.* **1984**, *16*, 307–347. (b) Toniolo, C.; Benedetti, E. *ISI Atlas Sci.: Biochem.* **1988**, *1*, 225. (c) Karle, I. L.; Balaram, P. *Biochemistry* **1990**, *29*, 6747–6756. (d) Toniolo, C.; Benedetti, E. *Trends Biochem. Sci.* **1991**, *16*, 350–353. (e) Kaul, R. K.; Balaram, P. *Bioorg. Med. Chem.* **1999**, *7*, 105–117. (f) Venkatraman, J.; Shankaramma, S. C.; Balaram, P. *Chem. Rev.* **2001**, *101*, 3131–3152.
- (2) (a) The definition of backbone dihedral angles follows the IUPAC-IUB Commission on Biochemical Nomenclature. *J. Mol. Biol.* **1970**, *52*, 1–17. α_L refers to *left-handed* $3_{10}/\alpha$ helical conformations while α_R denotes a *right-handed* helical conformation. Since both 3_{10} and α -helical conformations fall in a limited region of ϕ, ψ space, the terms α_L and α_R are used in a generic sense. (b) All the amino acids are of L chirality unless otherwise specified. (c) Abbreviations used: Aib = α -aminoisobutyric acid; Boc = tertiary butyloxycarbonyl; OMe = methyl ester; HPLC = high performance liquid chromatography.

- (3) (a) Gurunath, R.; Balaram, P. *Biochem. Biophys. Res. Commun.* **1994**, *202*, 241–245. (b) Fairman, R.; Anthony-Cahill, S. J.; DeGrado, W. F. *J. Am. Chem. Soc.* **1992**, *114*, 5458–5459. (c) Rothemund, S.; Beyermann, M.; Krause, E.; Krause, G.; Bienert, M.; Hodges, R. S.; Sykes, B. D.; Sönnichsen, F. D. *Biochemistry* **1995**, *34*, 12954–12962. (d) Chen, Y.; Mant, C. T.; Hodges, R. S. *J. Pept. Res.* **2002**, *59*, 18–33. (e) Aravinda, S.; Shamala, N.; Desiraju, S.; Balaram, P. *Chem. Commun.* **2002**, 2454–2455.
- (4) Schellman, C. In *Protein Folding*; Jaenicke, R., Ed.; Elsevier/North-Holland Biochemical Press: Amsterdam, 1980; pp 53–61.
- (5) (a) Milner-White, E. J. *J. Mol. Biol.* **1988**, *199*, 915–930. (b) Nagarajaram, H. A.; Sowdhamini, R.; Ramakrishnan, C.; Balaram, P. *FEBS Lett.* **1993**, *321*, 79–83. (c) Aurora, R.; Srinivasan, R.; Rose, G. D. *Science* **1994**, *264*, 1126–1130. (d) Gunasekaran, K.; Nagarajaram, H. A.; Ramakrishnan, C.; Balaram, P. *J. Mol. Biol.* **1998**, *275*, 917–932.

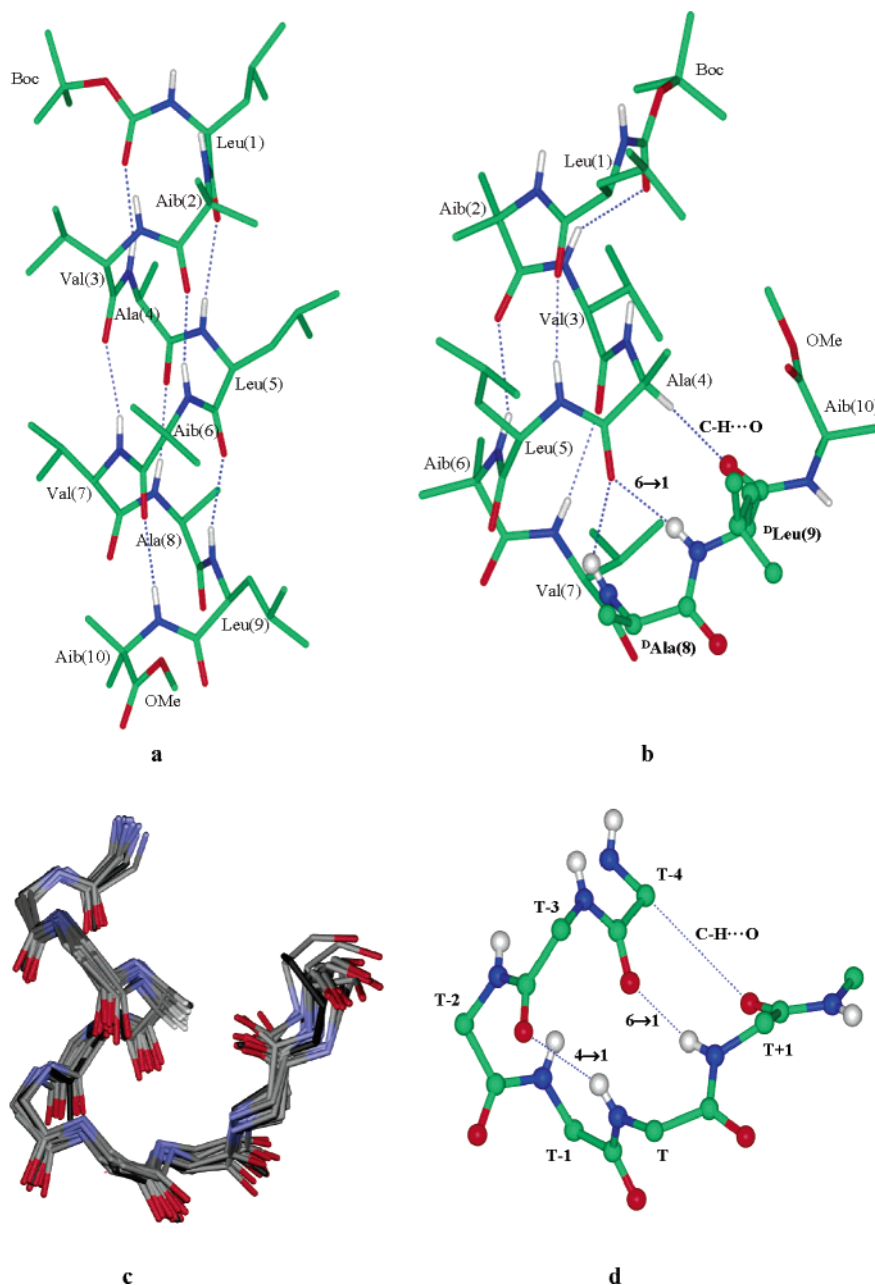


Figure 1. (a) Molecular conformation in crystals of Boc-Leu-Aib-Val-Ala-Leu-Aib-Val-Ala-Leu-Aib-OMe. Note the formation of an almost perfect α -helix.⁷ (b) Molecular conformation in crystals of Boc-Leu-Aib-Val-Ala-Leu-Aib-Val-^DAla-^DLeu-Aib-OMe **1**. Note unusual chain reversal stabilized by the Ala(4)^CH \cdots OC ^DLeu(9) hydrogen bond.⁸ (c) Superposition of 15 structures extracted from the Protein Data Bank which reveal a close similarity to the helix terminating motif observed in peptide **1** (from ref 9a). (d) A representation of the helix terminating motif identifying the stabilizing hydrogen bonds. Note nomenclature used for the residues along the polypeptide chain: T corresponds to the helix terminating residue, which adopts an α_L conformation.

Aib-Val-Ala-Leu-Aib-Val-Ala-Leu-Aib-OMe, which folded into a perfect α -helical conformation stabilized by seven 5 \rightarrow 1 hydrogen bonds (Figure 1a).⁷ This sequence was chosen as the template for the site specific introduction of D-residues. During

the course of our studies, we encountered an unusual reversal of polypeptide chain direction at the C-terminus of a synthetic decapeptide helix Boc-Leu-Aib-Val-Ala-Leu-Aib-Val-^DAla-^DLeu-Aib-OMe **1**, which appeared to be stabilized by an unusual C-H \cdots O hydrogen bond, between Ala(4)^CH and ^DLeu(9) CO groups (Figure 1b).⁸ We subsequently examined a dataset of 634 high-resolution protein structures in order to identify similar helix terminating motifs in proteins. A total of 111 examples were identified.⁹ The superposition of 15 examples with the structure of peptide **1** is shown in Figure 1c. It thus appeared that the C-H \cdots O hydrogen bond between T-4 ^CH and T+1 CO groups (where T is defined as the helix terminating residue

(6) For examples in designed peptides, see: (a) Karle, I. L.; Flippen-Anderson, J. L.; Uma, K.; Balaram, P. *Int. J. Pept. Protein Res.* **1993**, *42*, 401–410. (b) Di Blasio, B.; Pavone, V.; Saviano, R.; Fattorusso, C.; Pedone, E.; Benedetti, E.; Crisma, M.; Toniolo, C. *Pept. Res.* **1994**, *7*, 55–59. (c) Banerjee, A.; Datta, S.; Pramanik, A.; Shamala, N.; Balaram, P. *J. Am. Chem. Soc.* **1996**, *118*, 9477–9483. (c) Datta, S.; Shamala, N.; Banerjee, A.; Pramanik, A.; Bhattacharjya, S.; Balaram, P. *J. Am. Chem. Soc.* **1997**, *119*, 9246–9251. (d) Datta, S.; Uma, M. V.; Shamala, N.; Balaram, P. *Biopolymers* **1999**, *50*, 13–22. (e) Karle, I. L. *Biopolymers (Peptide Science)* **2001**, *60*, 351–365.

(7) Datta, S. *Folding of the Designed Peptides: X-ray Crystallographic Studies on the Structure, Conformation, Aggregation and Interactions of Oligopeptides Containing Conformationally Constrained Amino Acids*. Ph.D. Thesis, Indian Institute of Science, Bangalore, India, 1998.

(8) Aravinda, S.; Shamala, N.; Pramanik, A.; Das, C.; Balaram, P. *Biochem. Biophys. Res. Commun.* **2000**, *273*, 933–936.

Table 1. Data Collection and Refinement Parameters for Peptides **2**, **3**, and **4** Boc-Leu-Aib-Val-**Xxx**-Leu-Aib-Val-^DAla-^DLeu-Aib-OMe (**Xxx** = Gly **2**; ^DAla **3**; Aib **4**)

	peptide 2	peptide 3	peptide 4
empirical formula	C ₅₁ H ₉₂ N ₁₀ O ₁₃ ·H ₂ O	C ₅₂ H ₉₄ N ₁₀ O ₁₃ ·3H ₂ O	C ₅₃ H ₉₆ N ₁₀ O ₁₃ ·H ₂ O
crystal habit	clear and thin plates	clear and rectangular plates	clear and thin plates
crystal size (mm ³)	0.4 × 0.23 × 0.04	0.4 × 0.3 × 0.2	0.32 × 0.1 × 0.04
crystallizing solvent	methanol/water	ethanol/ethyl acetate	methanol/dioxane/water
space group	P2 ₁ 2 ₁ 2 ₁	P4 ₃ 2 ₁ 2	C222 ₁
cell parameters			
<i>a</i> (Å)	13.818(2)	25.115(4)	20.185(6)
<i>b</i> (Å)	21.595(9)	25.115(4)	30.163(8)
<i>c</i> (Å)	21.928(8)	43.709(10)	25.969(10)
α (deg)	90.0	90.0	90.0
β (deg)	90.0	90.0	90.0
γ (deg)	90.0	90.0	90.0
volume (Å ³)	6543(4)	27570(9)	15811(9)
<i>Z</i>	4	16	8
molecules/asym. unit	1	2	1
cocrystallized solvent	H ₂ O	3 H ₂ O	H ₂ O
molecular weight	1053.35 + 18	1067.37 + 54	1081.4 + 18
density (g/cm ³)	1.069	1.052	0.922
<i>F</i> (000)	2288	9472	4768
radiation	Cu K α (λ = 1.5418 Å)	Mo K α (λ = 0.7107 Å)	Mo K α (λ = 0.7107 Å)
temperature (°C)	21	21	21
2 θ max (deg)	110	54.2	46.52
scan type	ω – 2 θ	ω	ω
scan speed	variable		
measured reflections		355 061	48 890
independent reflections	4559	29 024	11 301
unique reflections	4559	16 061	6127
observed reflections [<i>F</i> > 4 σ (<i>F</i>)]	2428	6693	4967
final R (%)	10.6	6.99	10.64
final wR2 (%)	23.7	15.7	18.54
goodness-of-fit	1.13	0.795	0.960
$\Delta\rho_{\max}$ (e Å ⁻³)	0.31	0.35	0.28
$\Delta\rho_{\min}$ (e Å ⁻³)	-0.27	-0.18	-0.27
no. of restraints/parameters	0/675	4/1378	16/684
data-to-parameter ratio	3.6:1	4.8:1	7.2:1

adopting an α_L conformation, Figure 1d) appears to be an important determinant of the structure.

C–H···O hydrogen bonds have been widely implicated as important structural determinants in organic crystals¹⁰ and biological macromolecules.¹¹ Extensive theoretical calculations suggests that C–H···O interactions may be distinctly weaker than their N–H···O or O–H···O counterparts.¹² Some recent studies suggest that C–H···O interactions may have appreciable

magnitudes with a study of DMF dimers yielding a hydrogen bond energy of -3.0 ± 0.5 kcal/mol for the C–H···O interaction.^{12b} Similar estimates have been reported for hydrogen bonds between a water oxygen atom acceptor and C α –H donors in amino acid residues.^{12c} These theoretical estimates point to a possible structure determining role for C–H···O interactions. In the case of many weak interactions observed in crystal structures, the question often arises as to whether an optimum geometrical arrangement of the interacting atoms is a consequence or determinant of the structure. The problem of deciding whether short interatomic contacts observed in crystals are stabilizing has been specifically addressed with respect to the appearance of polymorphic forms in molecular crystals. Dunitz and Gavezzotti while analyzing 1,4-dichlorobenzene polymorph crystals have cautioned that: “The contact atom pairs that occur in molecular crystals should not necessarily be considered as the prime promoters of the intermolecular attraction but rather as a result of long-range effects”.¹³ If we extend this admonition to intramolecular interactions such as that observed in peptide **1**, it becomes necessary to gather further evidence for supporting the role ascribed to the intramolecular C–H···O hydrogen bond.⁸ The unusual conformation in peptide **1** suggests that the C–H···O interaction shown in Figure 1b is indeed a determinant of the structure, a conclusion reached in view of the absence of any other obviously stabilizing interactions. To further delineate the role of the C–H···O hydrogen bond, we have determined the crystal structures of three related decapeptide sequences (**2**–**4**), in which systematic replacements have been made at residue 4.

Boc-Leu-Aib-Val-**Ala**-Leu-Aib-Val-^DAla-^DLeu-Aib-OMe (**1**)

Boc-Leu-Aib-Val-**Gly**-Leu-Aib-Val-^DAla-^DLeu-Aib-OMe (**2**)

Boc-Leu-Aib-Val-^D**Ala**-Leu-Aib-Val-^DAla-^DLeu-Aib-OMe (**3**)

Boc-Leu-Aib-Val-**Aib**-Leu-Aib-Val-^DAla-^DLeu-Aib-OMe (**4**)

The results establish the role of the C–H···O interaction in generating the unusual chain reversal at the C-terminus of polypeptide helices.

Experimental Procedures

Peptide Synthesis. Peptides **2**, **3**, and **4** were synthesized by conventional solution phase methods, using a fragment condensation strategy.¹⁴ The Boc-group was used for N-terminal protection, and the C-terminus was protected as a methyl ester. Deprotections were performed using 98% formic acid and saponification for N- and C-terminus, respectively. Couplings were mediated by dicyclohexylcarbodiimide/1-hydroxybenzotriazole (DCC/HOBT). All the intermediates were characterized by ¹H NMR (80 MHz) and thin-layer chromatography (TLC) on silica gel and used without further purification. The final peptides were purified by medium-pressure liquid chromatography (MPLC) on a C₁₈ reverse phase column using methanol–water gradients. The peptides were further purified by reverse phase HPLC on a C₁₈ (5–10 μ) column using methanol–water gradients. The purified peptides were analyzed by electrospray mass spectrometry. (*M*_{cal} = 1053.2, *M*_{obs} = 1077.2 [M + Na⁺] for peptide **2**; *M*_{cal} = 1067.2, *M*_{obs} = 1091.2 [M + Na⁺] for peptide **3**; *M*_{cal} = 1081.2, *M*_{obs} = 1105.2 [M + Na⁺] for peptide **4**).

- (9) (a) Madan Babu, M.; Kumar Singh, S.; Balam, P. *J. Mol. Biol.* **2002**, *322*, 871–880. For the possible relevance of this motif in aligning helices and sheets in antiparallel fashion in protein, see: (b) Kumar Singh, S.; Madan Babu, M.; Balam, P. *Proteins: Struct., Funct., Genet.* **2003**, *51*, 167–171.
- (10) (a) Desiraju, G. R. *Acc. Chem. Res.* **1996**, *29*, 441–449. (b) Steiner, T. *Chem. Commun.* **1997**, 727–734. (c) Desiraju, G. R.; Steiner, T. *The Weak Hydrogen Bond in Structural Chemistry and Biology*; Oxford University Press: Oxford, 1999. (d) Desiraju, G. R. *Crystal Engineering. The Design of Organic Solids*; Elsevier: Amsterdam, 1989. (e) Steiner, T. *Angew. Chem., Int. Ed.* **2002**, *41*, 48–76.
- (11) (a) Derewenda, Z. S.; Lee, L.; Derewenda, U. *J. Mol. Biol.* **1995**, *252*, 248–262. (b) Fabiola, G. F.; Krishnaswamy, S.; Nagarajan, V.; Pattabhi, V. *Acta Crystallogr., Sect. D* **1997**, *53*, 316–320. (c) Wahl, M. C.; Sundaralingam, M. *Trends Biochem. Sci.* **1997**, *22*, 97–102. (d) Chakrabarti, P.; Chakrabarti, S. *J. Mol. Biol.* **1998**, *284*, 867–873.

- (12) (a) Gu, Y.; Kar, T.; Scheiner, S. *J. Am. Chem. Soc.* **1999**, *121*, 9411–9422. (b) Vargas, R.; Garza, J.; Dixon, D. A.; Hay, B. P. *J. Am. Chem. Soc.* **2000**, *122*, 4750–4755. (c) Scheiner, S.; Kar, T.; Gu, Y. *J. Biol. Chem.* **2001**, *276*, 9832–9837.
- (13) Dunitz, J. D.; Gavezzotti, A. *Helv. Chim. Acta* **2002**, *85*, 3949–3964.
- (14) Balam, H.; Sukumar, M.; Balam, P. *Biopolymers* **1986**, *25*, 2209–2223.

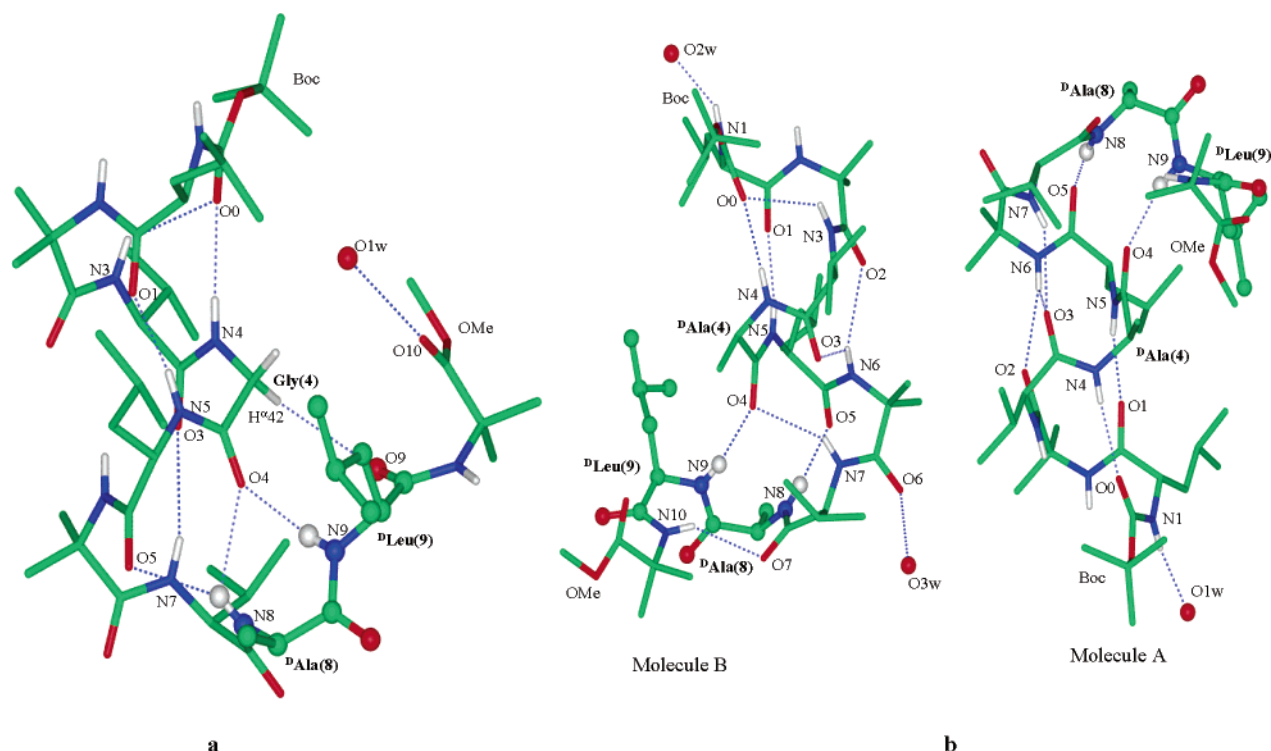


Figure 2. (a) Molecular conformation in crystals of Boc-Leu-Aib-Val-Gly-Leu-Aib-Val-^DAla-^DLeu-Aib-OMe **2**. (b) Molecular conformation in crystals of Boc-Leu-Aib-Val-^DAla-Leu-Aib-Val-^DAla-^DLeu-Aib-OMe **3**. Two independent molecules are observed in the crystallographic asymmetric unit. The atoms of the double *D*-segment are shown in ball-and-stick representation for easy identification.

Table 2. Torsion Angles (deg)^a

residue	peptide 2(1) Xxx = Gly(Ala)			peptide 3 Xxx = ^D Ala						peptide 4 Xxx = Aib		
	ϕ	ψ	ω	molecule A		molecule B		ϕ	ψ	ω	ϕ	ψ
Leu(1)	-65.3(-67) ^b	-29.5(-18)	-178.7	-59.6 ^b	-40.5	-175.7	-64.4 ^b	-42.2	180	-57.3 ^b	-39.1	-174.9
Aib(2)	-55.7(-51)	-42.2(-45)	-179.2	-52.3	-48.8	-178.1	-49.4	-47.1	-177.4	-57.7	-34.3	174.4
Val(3)	-79.9(-69)	-46.1(-44)	179.7	-72.0	-41.4	177.2	-69.5	-44.2	179.2	-80.8	-44.9	-175.8
Xxx(4)	-60.2(-55)	-44.3(-45)	-176.6	-46.6	-52.9	-177.3	-54.1	-48.6	-176.6	-53.0	-41.1	-173.1
Leu(5)	-64.5(-68)	-38.8(-44)	-179.9	-65.5	-43.9	-175.0	-62.6	-39.6	-177.3	-101.8	7.1	173.2
Aib(6)	-56.0(-59)	-39.0(-45)	-172.9	-55.6	-32.6	-177.4	-57.7	-30.0	-178.6	51.6	42.8	-179.4
Val(7)	-96.8(-107)	-8.5(-7)	-176.9	-106.6	25.1	164.3	-111.9	27.1	164.3	42.5	40.0	178.6
^D Ala(8)	85.1(84)	30.8(42)	167.8	76.8	21.4	178.1	67.8	30.1	176.7	66.8	15.7	179.9
^D Leu(9)	126.8 (130)	-155.7(-160)	-163.6	90.4	14.8	176.2	72.1	21.1	179.0	84.7	35.0	159.0
Aib(10)	51.5(51)	-146.2(-149) ^c	179.1 ^d	-40.3	-51.8 ^c	-173.7 ^d	-46.6	151.2 ^c	166.5 ^d	49.5	-145.0 ^c	-167.2 ^d
side chain	χ^1	χ^2	χ^1	χ^2	χ^1	χ^2	χ^1	χ^2	χ^1	χ^2	χ^1	χ^2
Leu(1)	-69.4	-70.2, 171.8	-178.4	63.6, -172.6	-179.4	56.4, 175.7	-162.6	72.9, -160.2				
Val(3)	-60.0, 179.6	57.2, 178.8			-59.8, 171.5		-65.5, 173.5					
Leu(5)	-71.8	-74.7, 157.3	-70.1	-62.3, 176.7	-174.2	61.3, 173.9	-52.1	-55.8, -178.9				
Val(7)	-49.9, 71.1	62.7, 61.4			62.3, -67.0		41.2, -62.7					
^D Leu(9)	56.5	57.1, -177.4	67.1	48.8, -178.7	89.4	-55.4, 178.1	74.2	56.1, -175.2				

^a Torsion angles shown in bold correspond to the helix terminating (T) residue which adopts an α_L conformation. ^b C'(0)-N(1)-C α (1)-C'(1). ^c N(10)-C α (10)-C'(10)-O(OMe). ^d C α (10)-C'(10)-O(OMe)-C(OMe).

X-ray Diffraction. X-ray diffraction data were collected on a CAD4 diffractometer (Cu K α) for peptide **2** and on a Bruker AXS SMART APEX CCD diffractometer (Mo K α) for peptides **3** and **4**. Crystal, diffraction data, and refinement details are summarized in Table 1.

Boc-Leu-Aib-Val-Gly-Leu-Aib-Val-^DAla-^DLeu-Aib-OMe (2). The structure was solved by direct methods using the Shake-and-Bake method¹⁵ (SnB), which uses minimal-function phase refinement and a Fourier filtering procedure. This gave a fragment containing 45 atoms, which was then used in the partial structure expansion method, employing 200 reflections satisfying the criterion $E_{\text{obs}} \geq 1.5$ and the largest $E_{\text{calc}}/E_{\text{obs}}$. The Fourier map generated with the improved phase

set revealed 73 out of 74 non-hydrogen atoms in the asymmetric unit. The remaining atoms were located from difference Fourier maps. The structure was refined isotropically followed by full matrix anisotropic least-squares refinement using SHELXL-97.¹⁶ All the hydrogen atoms were fixed geometrically in idealized positions and allowed to ride with the C or N atom to which each was bonded in the final cycle of refinement. The final *R* factor was 10.6%.

Boc-Leu-Aib-Val-^DAla-Leu-Aib-Val-^DAla-^DLeu-Aib-OMe (3) and Boc-Leu-Aib-Val-Aib-Leu-Aib-Val-^DAla-^DLeu-Aib-OMe (4). The structures were solved by direct methods using SHELXD.¹⁷ For **3**, two fragments were obtained containing 72 and 70 atoms. Remaining atoms

(15) Miller, R.; Gallo, S. M.; Khalal, H. G.; Weeks, M. C. *J. Appl. Crystallogr.* **1994**, *27*, 613–621.

(16) Sheldrick, G. M. *SHELXL-97, Program for the Refinement of Crystal Structures*. Universität Göttingen: Germany, 1997.

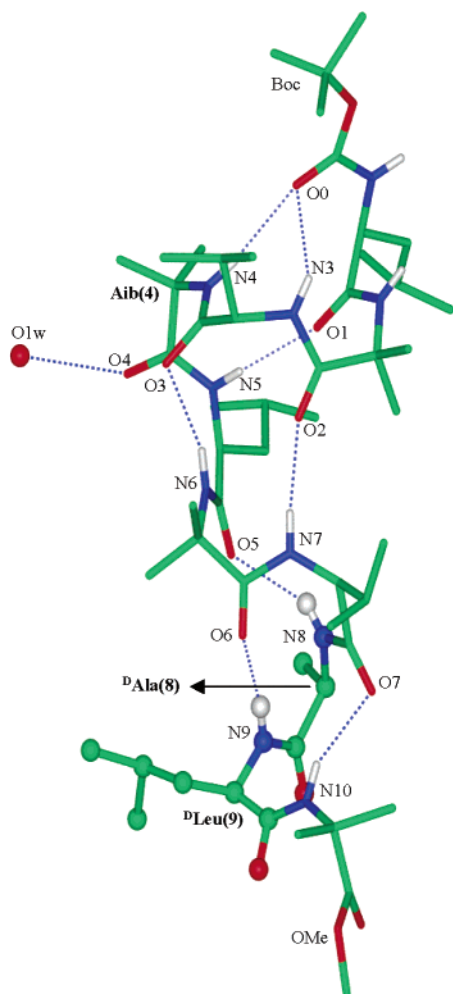


Figure 3. Molecular conformation in crystals of Boc-Leu-Aib-Val-Aib-Leu-Aib-Val-DAla-DLeu-Aib-OMe **4**. The atoms of the double D-segment are shown in ball-and-stick representation for easy identification.

Table 3. Hydrogen Bonds in Peptide 2

type	donor	acceptor	N···O (Å)	H···O (Å)	C=O···H (deg)	C=O···N (deg)	O···HN (deg)
Intermolecular							
solvent	N(1)	O(8) ^a	2.957	2.101	106.3	107.6	172.9
	N(2)	O(7) ^a	2.995	2.185	125.0	127.1	157.0
	N(10)	O(6) ^b	2.867	2.027	141.6	145.5	165.2
	O1w	O(10)	2.803				
Intramolecular							
4 → 1	N(3)	O(0)	3.123	2.489	120.7	129.5	131.2
5 → 1	N(4)	O(0)	2.992	2.140	147.0	149.6	170.4
5 → 1	N(5)	O(1)	2.794	1.950	143.4	147.0	166.6
5 → 1	N(7)	O(3)	3.334	2.573	154.4	161.5	148.1
5 → 1	N(8)	O(4)	2.996	2.450	145.0	158.5	122.0
4 → 1	N(8)	O(5)	3.308	2.548	95.2	103.1	148.0
6 → 1	N(9)	O(4)	2.803	2.011	145.9	142.5	152.8

^a Symmetry related by $x + 1, y, z$. ^b Symmetry related by $-x - 1/2, -y + 1, z + 1/2$.

were located from difference Fourier maps. The structures were refined isotropically followed by full matrix anisotropic least-squares refinement using SHELXL-97. All the hydrogen atoms were fixed geometrically in the idealized position and allowed to ride with the C or N atom to which each was bonded for the final cycle of refinement. The final *R* factor was 6.9%.

For **4**, a fragment containing 63 atoms was obtained. The remaining atoms were located from difference Fourier maps. Refinement was

Table 4. Hydrogen Bonds in Peptide 3

Molecule A							
type	donor	acceptor	N···O (Å)	H···O (Å)	C=O···H (deg)	C=O···N (deg)	O···NH (deg)
Intermolecular							
solvent	N(2)	O(9) ^a	2.897	2.142	150.0	159.3	146.4
	O1w	O(8) ^a	2.710				
	O2w	O(7) ^b	3.104				
	N(1)	O1w	2.858	2.076			167.2
Intramolecular							
5 → 1	N(4)	O(0)	3.068	2.221	151.8	154.1	168.4
5 → 1	N(5)	O(1)	2.874	2.028	165.3	165.9	167.4
5 → 1	N(6)	O(2)	3.218	2.416	137.2	143.4	155.4
5 → 1	N(7)	O(3)	3.258	2.495	155.7	161.8	148.2
4 → 1	N(8)	O(5)	2.941	2.093	112.5	114.2	168.8
6 → 1	N(9)	O(4)	2.912	2.076	151.3	147.6	163.9
4 → 1 ^e	N(10)	O(7)	3.565	2.789	107.1	113.5	150.9
Molecule B							
type	donor	acceptor	N···O (Å)	H···O (Å)	C=O···H (deg)	C=O···N (deg)	O···NH (deg)
Intermolecular							
solvent	N(2)	O(9) ^c	2.945	2.127	146.0	151.7	158.7
	O2w	O(8) ^c	3.106				
	O1w ^d	O(8) ^c	2.760				
	O2w	O1w ^d	3.315				
	N(1)	O2w	2.830	2.066			147.6
solvent	O3w	O(6)	3.217				
Intramolecular							
4 → 1	N(3)	O(0)	3.119	2.559	117.8	128.2	123.7
5 → 1	N(4)	O(0)	3.064	2.215	153.2	155.7	169.0
5 → 1	N(5)	O(1)	2.885	2.035	163.1	164.9	169.9
5 → 1	N(6)	O(2)	3.234	2.474	135.5	142.9	147.8
4 → 1	N(6)	O(3)	3.103	2.588	97.8	111.1	119.5
4 → 1	N(7)	O(4)	3.281	2.570	104.9	113.7	140.6
4 → 1	N(8)	O(5)	2.973	2.127	109.8	111.6	167.8
6 → 1	N(9)	O(4)	3.010	2.166	145.3	143.5	166.8
4 → 1	N(10)	O(7)	3.276	2.513	115.1	122.5	148.3

^a Symmetry related by $x + 1/2, -y + 3/2, -z + 1/4$. ^b Symmetry related by $x + 1/2, -y + 1/2, -z + 1/4$. ^c Symmetry related by $x - 1/2, -y + 1/2, -z + 1/4$. ^d Symmetry related by $x, y - 1, z$. ^e This interaction is listed despite relatively long N···O and H···O distances.

Table 5. Hydrogen Bonds in Peptide 4

type	donor	acceptor	N···O (Å)	H···O (Å)	C=O···H (deg)	C=O···N (deg)	O···HN (deg)
Intermolecular							
solvent	N(1)	O(4) ^a	2.987	2.132	132.8	134.2	172.1
	N(2)	O1w ^a	3.072	2.290			151.3
	O1w	O(4)	3.043				
Intramolecular							
4 → 1	N(3)	O(0)	3.200	2.557	114.8	124.1	132.3
5 → 1	N(4)	O(0)	3.189	2.340	156.2	159.1	169.4
5 → 1	N(5)	O(1)	3.030	2.232	155.0	160.1	154.3
4 → 1	N(6)	O(3)	3.127	2.306	105.8	111.0	159.9
6 → 1	N(7)	O(2)	3.008	2.196	151.3	153.5	157.5
4 → 1	N(8)	O(5)	3.035	2.261	125.5	132.4	149.7
4 → 1	N(9)	O(6)	2.987	2.155	130.4	135.2	162.8
4 → 1	N(10)	O(7)	3.108	2.298	110.9	116.5	157.0

^a Symmetry related by $x + 1/2, -y + 1/2, -z + 1$.

carried out with full matrix least-squares methods using SHELXL-97. All non-hydrogen atoms were initially refined isotropically followed by full matrix anisotropic least-squares refinement. During the course of refinement, the atoms C1' and COM showed nonpositive definite temperature factors. Hence, they were included in subsequent refinement with isotropic temperature factors. All the hydrogen atoms were fixed geometrically in the idealized positions and allowed to ride with the C or N atom to which each was bonded for the final cycle of refinement. The final *R* factor was 10.64%.

Results and Discussion

Peptide Conformation. The molecular conformations of peptide **2–4** in crystals are illustrated in Figures 2 and 3. The

(17) Schneider, T. R.; Sheldrick, G. M. *Acta Crystallogr.* **2002**, *D58*, 1772–1779.

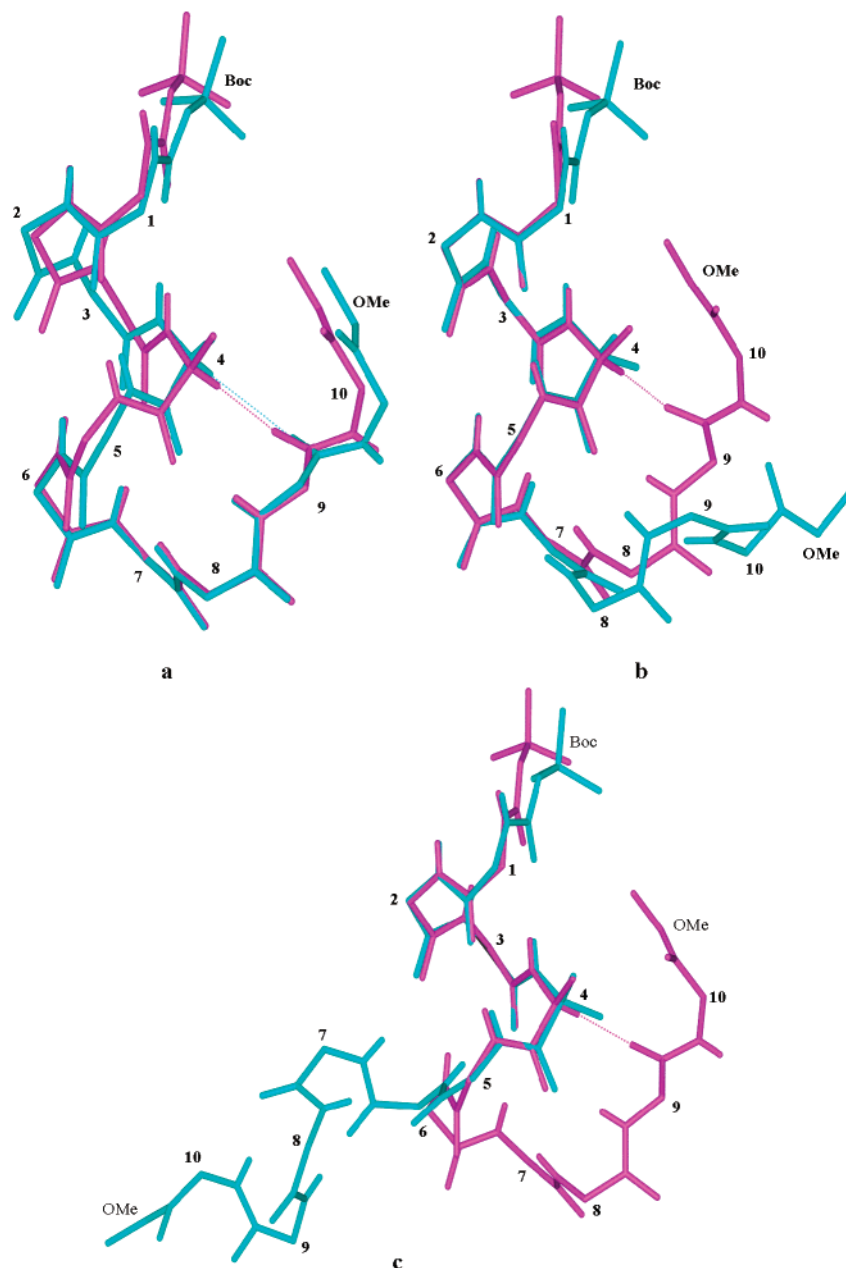


Figure 4. Superposition of decapeptide structures in pairs highlighting conformational similarities and differences. (a) Peptides **1** and **2** (rmsd = 0.54 Å for all the backbone atoms) (b) Peptides **1** and **3B** (rmsd = 0.347 Å for residues 1 to 7) (c) Peptides **1** and **4** (rmsd = 0.26 Å for residues 1 to 5).

backbone and side chain torsion angles are summarized in Table 2. The previously determined torsion angle for peptide **1** is also listed to facilitate direct comparison. Tables 3–5 list the intra- and intermolecular hydrogen bonds observed in the structures of the three peptides. Peptide **2** adopts a conformation very similar to that determined earlier for **1**. Residues 1 to 7 form a largely α -helical segment with a lone 3_{10} helical turn at the N-terminus. Helix termination occurs at D Ala(8), which adopts an α_L conformation. D Leu(9) adopts an extended conformation, facilitating the formation of a potentially stabilizing C–H \cdots O interaction between the *pro R* C $^{\alpha}$ H of Gly(4) and D Leu(9) CO group. The parameters for the C–H \cdots O interactions are C \cdots O = 3.599 Å, H \cdots O = 2.87 Å, \angle C–H \cdots O = 133.0°, and \angle H \cdots O=C = 132.5°. In the structure of peptide **1**, determined earlier,⁸ the corresponding parameters are C \cdots O = 3.271 Å, H \cdots O = 2.293 Å, \angle C–H \cdots O = 176.4°, and \angle C–H \cdots O

= 123.0°. The structures of peptides **1** and **2** could be superimposed, with an RMSD of 0.54 Å for all atoms (Figure 4a).

The replacement of Ala at residue 4 in peptide **1** by Gly in peptide **2** has therefore not influenced the folding of the backbone. In the case of Gly, there are two potential C $^{\alpha}$ –H bonds which can, in principle, participate in weak interactions. The comparison of peptides **1** and **2** suggests that *pro-R* hydrogen is optimally oriented in the observed conformation. We therefore turned to the structure of peptide **3** where residue 4 is D Ala. If D Ala is introduced at position 4, maintaining the observed conformation, the methyl group should disrupt the observed C–H \cdots O interaction. Peptide **3** crystallized with two independent molecules in the asymmetric unit (**3A**, **3B**), both of which adopted a *right-handed* helical conformation over the segment residues 1 to 7. Figure 4b shows the superposition of residues 1 to 7 for peptide **1** and **3B**, demonstrating the very

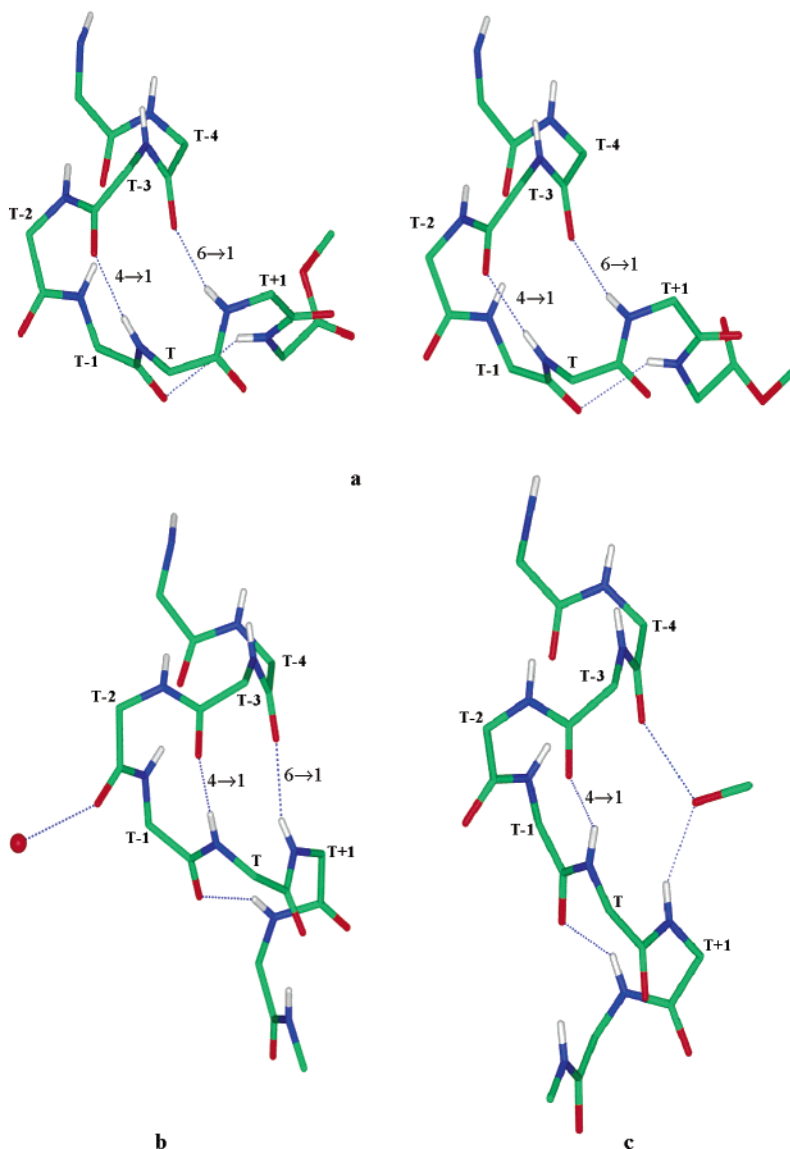


Figure 5. Comparison of helix terminating segments in peptides **3** and **4** and a related 14-residue peptide. Only backbone atoms are shown. (a) Two independent molecules in peptide **3**, T = ^DAla(8); (b) Peptide **4**, T = Aib(6); (c) Boc-L-(Val-Ala-Leu-Aib-Val-Ala-Leu)-D-(Val-Ala-Leu-Aib-Val-Ala-Leu)-OMe, T = ^DVal(8).^{5c} These examples provide a view of the junction between fused helical segments of opposite chirality. In the 14-residue peptide, solvent insertion into the 6→1 hydrogen bond in the helix terminating motif is observed.

close identity of the helical folds in the two peptides (rmsd = 0.342 Å). An interesting feature of the structure of peptide **3** is the occurrence of the ^DAla residue in the *right-handed* helical (α_R) conformation. Previous studies from our laboratory have demonstrated that even contiguous double D-segments can be accommodated in right-handed helical structures.^{3d} There is a dramatic difference in the conformation of the C-terminus residues in molecules **3A**, **3B** as compared to peptides **1** and **2**. ^DLeu(9) adopts an α_L conformation resulting in the formation of type I'/III' β -turn (3_{10} -helical turn) stabilized by a 4→1 hydrogen bond between the Val(7) CO and Aib(10) NH. This structure closely resembles the junction observed between fused right- and left-handed helices in designed peptides.

Having established the disruption of the C–H⋯O hydrogen bond structural motif, upon replacement of the appropriate C $^{\alpha}$ hydrogen at residue 4, we turn to the structure of peptide **4**, which contains an Aib residue at this position. The introduction of a C $^{\alpha,\alpha}$ disubstituted residue precludes any C–H⋯O interaction involving position 4. The molecular structure of **4** shows

dramatic changes from those observed for peptides **1**, **2**, and **3**. Inspection of the torsion angles in Table 2 immediately reveals that the right-handed helical segment is now considerably shorter. Figure 4c shows a superposition of the structures of **1** and **4** which illustrates the dramatic conformational change that accompanies replacement of Ala(4) in **1** with Aib(4) in **4**. Residues 1 to 5 form a short stretch of *right-handed* helix, with Aib(6) acting as the helix terminating residue, adopting an α_L conformation. Interestingly, residues 6 to 9 now form a *left-handed* helical structure. The conformation of the peptide can best be described as being composed of fused right- and left-handed helical segments, forming an ambidextrous helix. Such continuous helices of mixed chirality have been characterized earlier.^{5e,18} Figure 5 shows a comparison of helix terminating segments in peptides **3** and **4** with the junction between two helical blocks of opposite chirality in peptide Boc-L-(Val-Ala-Leu-Aib-Val-Ala-Leu)-D-(Val-Ala-Leu-Aib-Val-Ala-Leu)-

(18) Banerjee, A.; Raghobama, S.; Karle, I. L.; Balaram, P. *Biopolymers* **1996**, *39*, 279–285.

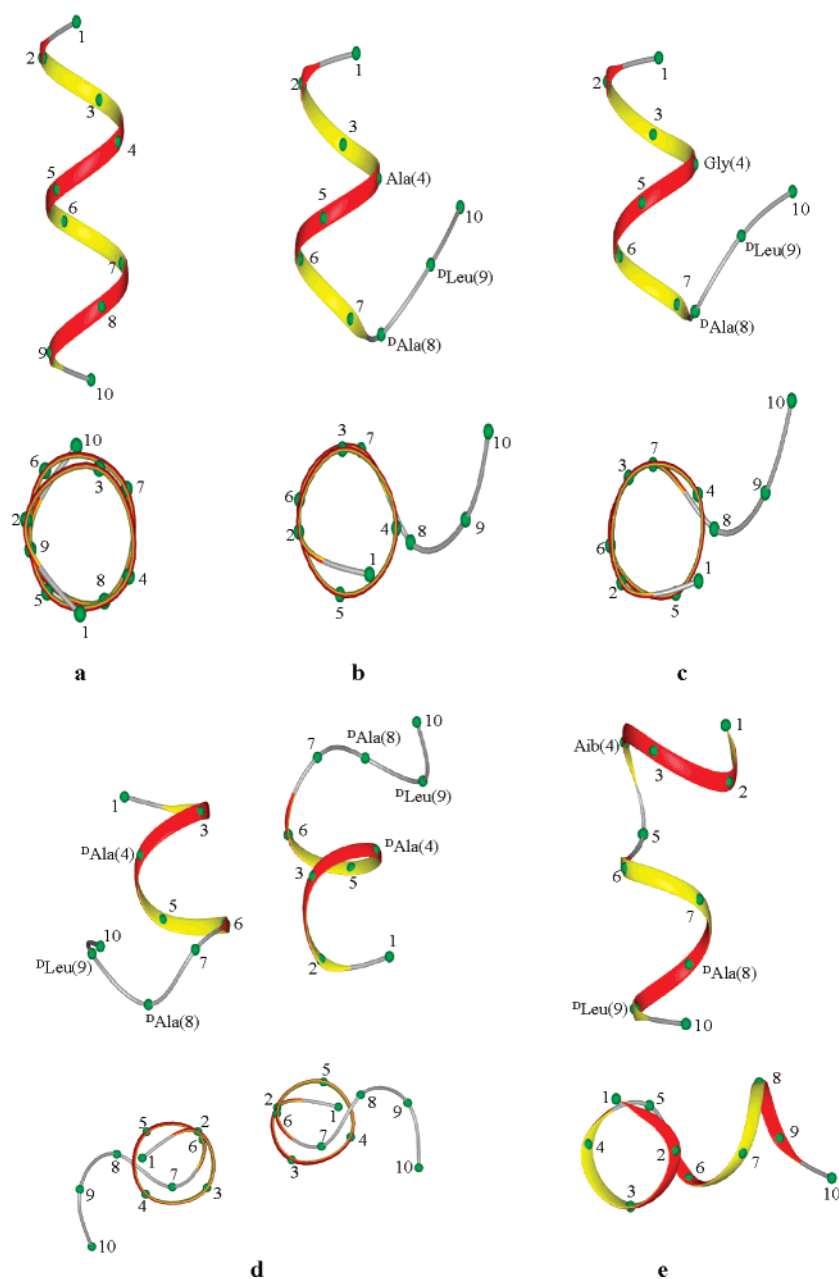


Figure 6. A schematic view of polypeptide helices. View in a direction perpendicular to the helix axis (top) and down the helix axis (bottom). (a) Boc-Leu-Aib-Val-Ala-Leu-Aib-Val-Ala-Leu-Aib-OMe (perfect α -helical conformation); (b) Boc-Leu-Aib-Val-Ala-Leu-Aib-Val-^DAla-^DLeu-Aib-OMe **2**; (c) Boc-Leu-Aib-Val-Gly-Leu-Aib-Val-^DAla-^DLeu-Aib-OMe **3**; (d) Boc-Leu-Aib-Val-^DAla-Leu-Aib-Val-^DAla-^DLeu-Aib-OMe **4**; (e) Boc-Leu-Aib-Val-Aib-Leu-Aib-Val-^DAla-^DLeu-Aib-OMe **5**.

OMe.^{5c} Figure 6 compares views of the peptide backbone-folding in peptides **1** to **4**. View in a direction approximately perpendicular to the helix axis and in a direction down the helix axis. For comparison, the perfect α -helical parent molecule Boc-Leu-Aib-Val-Ala-Leu-Aib-Val-Ala-Leu-Aib-OMe is also shown. These views clearly illustrate the role of the junction of opposite chirality in determining the direction of chain folding.

In the peptides **1–4**, helix termination occurs with the formation of a Schellman motif stabilized by a pair of hydrogen bonds of 6 \rightarrow 1 and 4 \rightarrow 1 types, although in peptide **1** the 4 \rightarrow 1 interaction appears relatively weak ($N\cdots O = 3.683 \text{ \AA}$, $H\cdots O = 2.973 \text{ \AA}$, and $\angle N-H\cdots O = 141.1^\circ$). In contrast, in peptide **4**, the Schellman motif is formed by residue 6(Aib) acting as the terminating residue. Here again, a pair of hydrogen bonds, 6 \rightarrow 1 and 4 \rightarrow 1, stabilized the formation of this motif. It is

important to note that the novel chain reversal in peptides **1** and **2** occurs after the Schellman motif and is primarily a consequence of the local conformation of the ^DLeu(9) residue. In principle, the ^DLeu(9) residue could have adopted an α_L conformation in peptides **1** and **2**, resulting in a structure almost identical to that observed in peptide **3**. Such a conformation would have indeed provided an additional intramolecular 4 \rightarrow 1 hydrogen bond between Val(7)CO and Aib(10) NH groups, as a consequence of the formation of an ^DAla(8)-^DLeu(9) type I' β -turn. Despite the availability of this favorable conformation, the peptide chain in molecules **1** and **2** folds back on the N-terminal helix, suggesting that the observed C-H \cdots O interaction together with other nonbonded forces determines the direction of peptide chain folding.

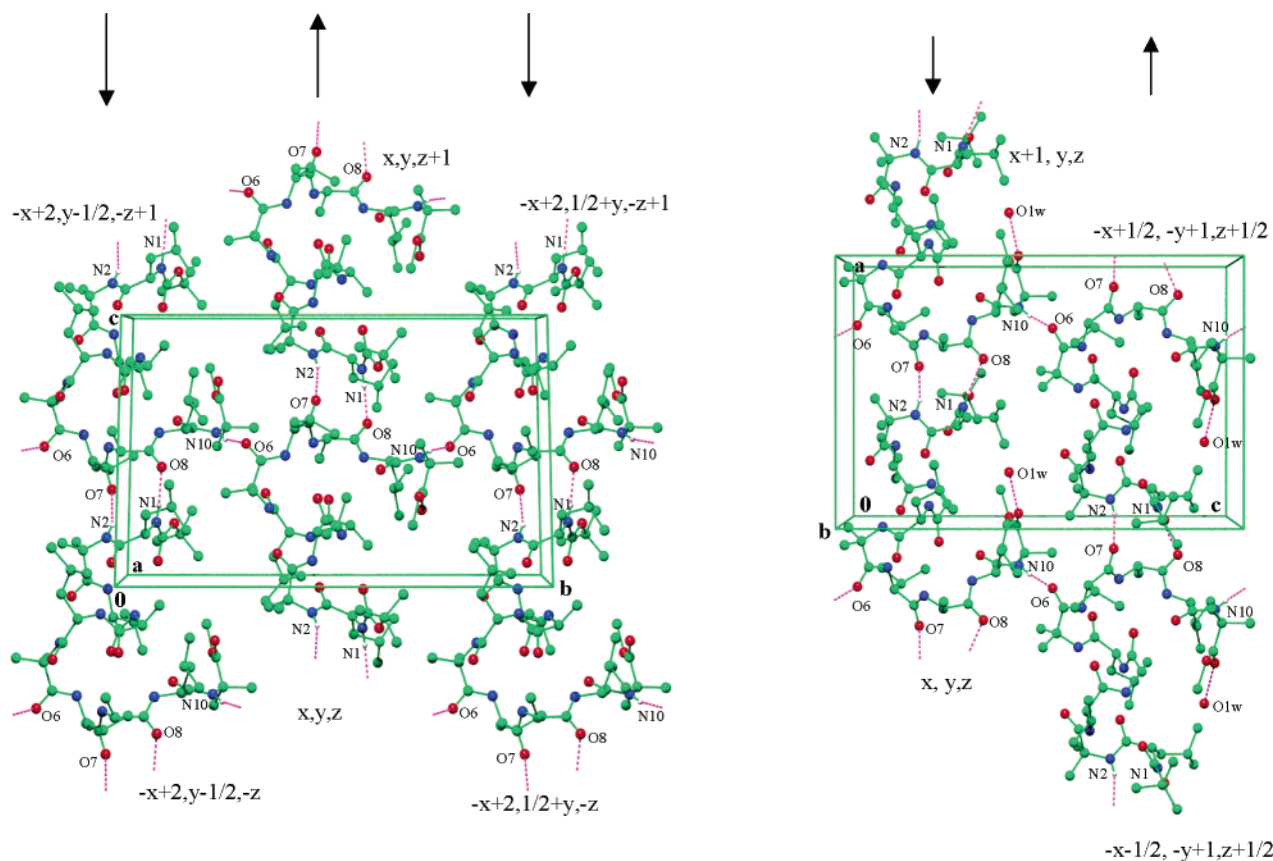


Figure 7. A view of the packing in crystals for peptides. (left) Boc-Leu-Aib-Val-Ala-Leu-Aib-Val-^DAla-^DLeu-Aib-OMe **1**, (right) Boc-Leu-Aib-Val-Gly-Leu-Aib-Val-^DAla-^DLeu-Aib-OMe **2**. Intermolecular hydrogen bonds are shown as dotted lines. Intramolecular hydrogen bonds are not indicated for the sake of clarity. Arrows indicate the direction of peptide chain propagation from the N-terminus to the C-terminus.

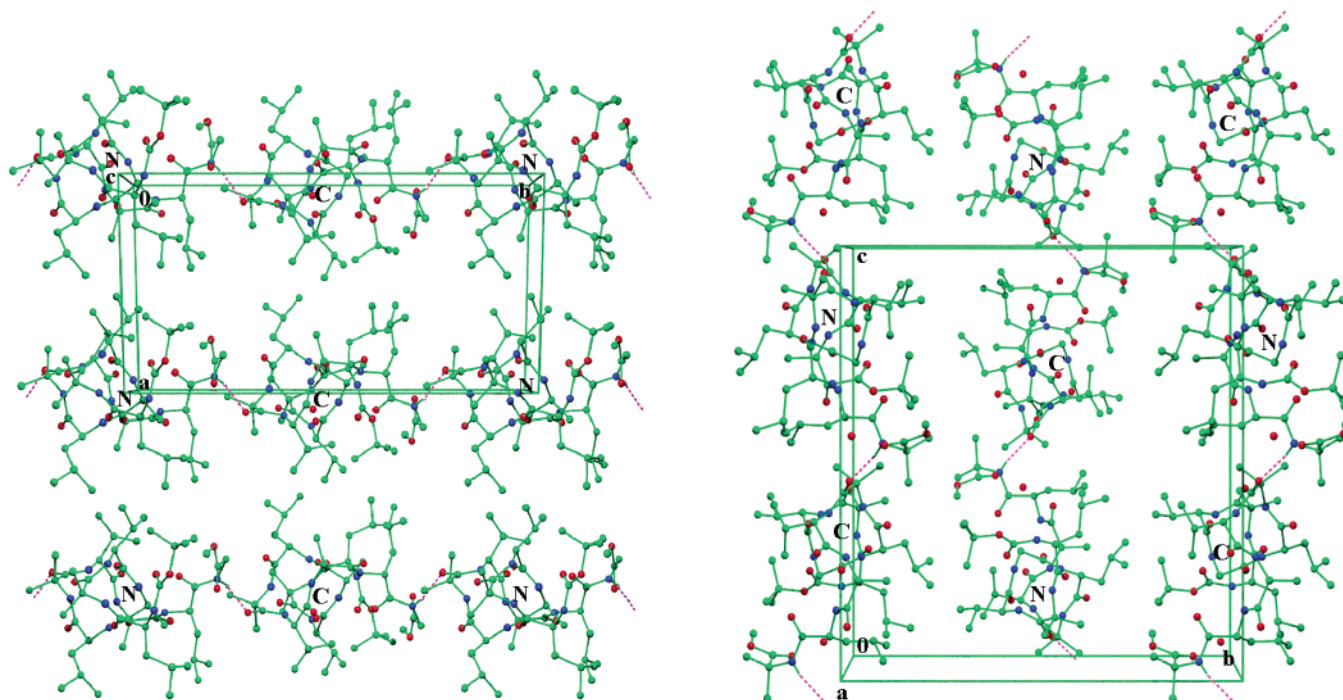


Figure 8. A view of the molecular packing in crystals for peptides **1** (left) and **2** (right), viewed down the long axis of the molecule. The direction of the peptide chain is indicated by the letters N and C. Alternating antiparallel columns are arranged in a square grid arrangement for **1** and a checkerboard arrangement for **2**.¹⁹

Crystal Packing. Inspection of the modes of packing of peptides **1** to **4** in crystals may be relevant in assessing the possible contributions of intermolecular interactions in influenc-

ing molecular conformation. Figure 7 shows a view of packing in peptides **1** and **2**. The bent molecules are held together in vertical columns, aligned parallel to the *a*-axis by a pair of

hydrogen bonds between exposed backbone amide groups (N(2)···O(7) and N(1)···O(8)). The adjacent columns are arranged in antiparallel fashion and connected laterally by the intermolecular hydrogen bond N(10)···O(6). A lone water molecule O1w fills a cavity between the peptides and forms only a single hydrogen bond to O(10) of the C-terminus ester group. Aib(6) NH does not participate in any hydrogen bond. The observation of a cavity filling water molecule with unsatisfied hydrogen bonding potential may be indicative of crystallization from an aggregate nucleus, composed of bent peptide molecules leading to imperfect packing. This suggests that the observed molecular conformation is not likely to be a consequence of strong intermolecular interactions that drive crystal formation. Peptide **1**, which adopts an almost similar conformation, crystallizes in the monoclinic space group $P2_1$ as compared to the orthorhombic $P2_12_12_1$ space group for peptide **2**. The mode of packing in crystals in peptide **1** is remarkably similar to that of peptide **2** (Figure 7), with all the three interpeptide hydrogen bonds being observed. The antiparallel columns are more closely arranged in peptide **1**, and the water molecule earlier observed in peptide **2** is absent in peptide **1**. The mode of aggregation in a direction perpendicular to the helix formed by residues 1 to 7 is shown in Figure 8. In peptide **1**, antiparallel columns, viewed down the axis of the molecule, form a square grid arrangement, while a checkerboard motif is observed in the case of peptide **2**.¹⁹ The view of molecular packing shown in Figures 7 and 8 do not reveal any specifically unusual feature, which may force the molecular conformation into the observed bent structure.

Peptides **3** and **4** may be viewed as structures generated by fused helical peptide segments of opposite chirality. In the case of **3**, the junction is between residues 7 and 8, with the resultant left-handed helical segment being restricted to only a single turn. In **4**, the junction occurs between residues 4 and 5 resulting in almost equal segments of right- and left-handed twist. The packing of these ambidextrous helices is mediated by two bridging water molecules in the case of peptide **3** and one bridging water molecule in peptide **4**. Crystals of **3** contain two molecules in the asymmetric unit. Figure 9 shows a close up view of the intermolecular interactions, which bridge molecules A and B in the lattice. A single interpeptide hydrogen bond between N(2)···O(9) holds columns of A molecules and B molecules in place. The two water molecules bridge the A and B columns and are also hydrogen bonded to one another.

In peptide **4**, the long axis of the molecule lies at an appreciable angle with respect to the crystallographic axis, with proximal helical units being bridged by both interpeptide and water mediated hydrogen bonds to the N-terminal NH groups, which are not involved in intramolecular hydrogen bonds. The observed intermolecular interaction involves both N(1) and N(2) (Table 5). Figure 10 shows a view of the molecular packing in peptide **4** down the c -axis. Interestingly, as many as three carbonyl groups (O(8), O(9), and O(10)) are not involved in hydrogen bonding. This imperfect pairing of hydrogen bond donors and acceptors in crystals once again suggests that crystal packing forces may not be a primary determinant of molecular conformation.

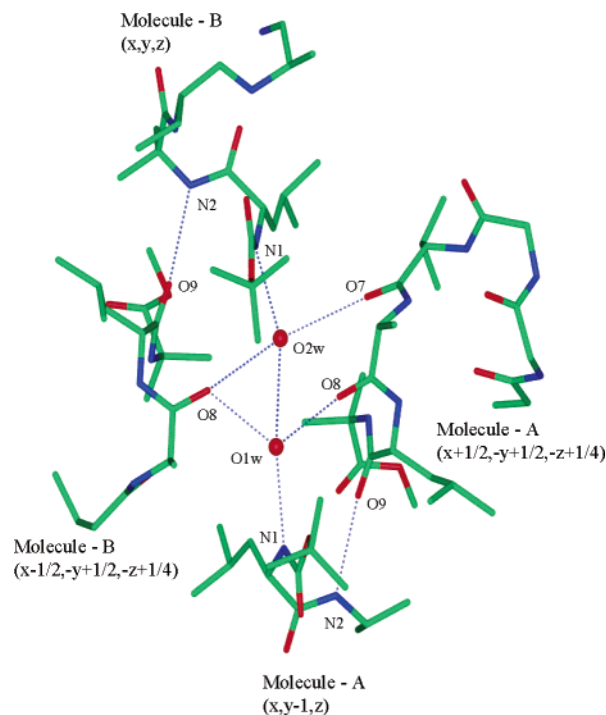


Figure 9. A view of the intermolecular interactions which bind molecules of peptide **3** in crystals. Two water molecules bridge peptide columns in both vertical and lateral directions. Note that the asymmetric unit contains two independent peptides labeled as molecules A and B.

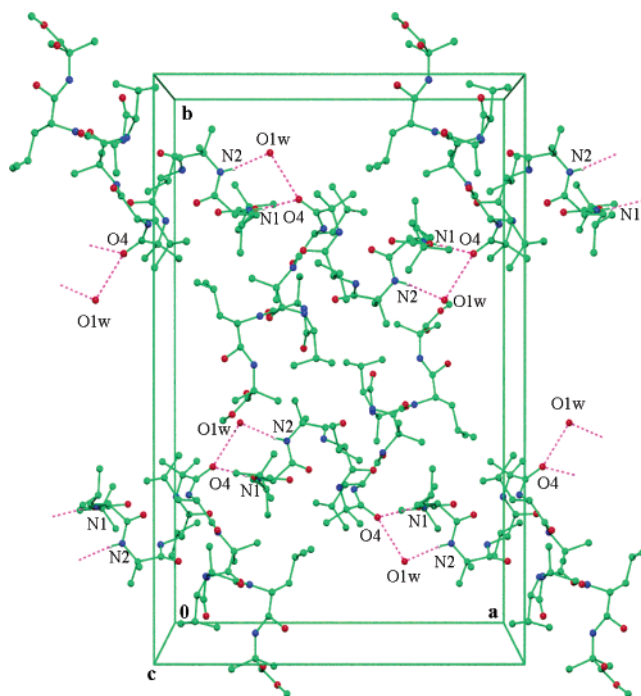


Figure 10. A view of the molecular packing in crystals for peptide **4**, down the crystallographic c -axis. The long axis of the molecule lies at an angle with respect to the crystallographic axes. Intermolecular hydrogen bonds mediating interaction between proximal molecules are shown as dotted lines.

Conclusion

The structures of peptides **1–4**, together with the structure of all the L decapeptide shown in Figure 1a, provide many insights into the nature of the interactions that determine the precise fold of designed peptides. The introduction of the double D-segment ^DAla(8)-^DLeu(9) clearly facilitates helix termination;

(19) (a) Karle, I. L. *Acta Crystallogr.* **1992**, *B48*, 341–356. (b) Karle, I. L. *Biopolymers* **1996**, *40*, 157–180. (c) Karle, I. L. *Acc. Chem. Res.* **1999**, *32*, 693–701.

when residue 4 is Ala or Gly, a novel chain reversal is observed at the C-terminus stabilized by the C–H···O hydrogen bond between residue 4 C^αH and residue 9 CO groups. This weak interaction appears to be a critical determinant of this unusual fold because the replacement of the interacting hydrogen by a methyl group results in a dramatic change in the conformation of the polypeptide. Thus, the T-4 C^αH···CO of T+1 interaction in α_L terminated segments in peptides and proteins undoubtedly contributes to the stability of a novel chain reversal which permits alignment of helical structures in adjacent extended sheets in antiparallel fashion.^{9b} Analysis of the modes of association of peptides **1** to **4** in crystals suggests that the observed molecular conformations may not be a consequence of crystal packing effects, but are determined by intramolecular interactions. The results presented in this paper provide firm evidence in support of the emerging view that C–H···O interactions may contribute significantly in energetic terms in determining folded structures in polypeptides and proteins.^{9,11}

Two serendipitous observations made during the course of these studies merit special mention. In peptide **3**, the ^DAla(4) residue adopts a *right-handed* (α_R) conformation, while, in peptide **4**, the ^LVal(7) residue adopts a *left-handed* (α_L) conformation. While amino acid chirality plays a dominant role

in determining the sense of the helix (L-amino acids favor a right-handed twist and D-amino acids favor a left-handed twist), the insertion of guest amino acids in folded sequences of opposite chirality does not necessarily lead to the disruption of the twist of the helical structures. Peptides **3** and **4** provide examples of the accommodation of amino acids of mixed chirality in a continuous helical segment. A detailed understanding of the role of chiral reversal on local conformational features of polypeptide chains promises to be useful in achieving control over backbone-folding in designed peptides.

Acknowledgment. This research was supported by a grant from the Council of Scientific and Industrial Research (N.S.) and program support in the area of drug and molecular design, Department of Biotechnology, India. The CCD diffractometer facility was supported under the IRPHA program of the Department of Science and Technology.

Supporting Information Available: X-ray crystallographic files for peptide **2–4** (CIF format). This material is available free of charge via the Internet at <http://pubs.acs.org>.

JA0372762